Liquid Crystals
Publication details, including instructions for authors and subscription information:
http://www.informaworld.com/smpp/title~content=t713926090

Different disk structures in the hexagonal columnar mesophases of 2,3-dicyano-6,7,10,11-tetraalkoxy-1,4-diazatriphenylenes and 2,3-dicyano-6,7,10,11-tetraalkoxytriphenylenes

Masahiro Ichihara[a]; Hiroomi Suzuki[a]; Bernhard Mohr[a]; Kazuchika Ohta[a]
[a] Smart Materials Science and Technology, Department of Bioscience and Textile Technology, Interdisciplinary Graduate School of Science and Technology, Shinshu University, 386-8567 Ueda, Japan

To cite this Article Ichihara, Masahiro , Suzuki, Hiroomi , Mohr, Bernhard and Ohta, Kazuchika(2007) 'Different disk structures in the hexagonal columnar mesophases of 2,3-dicyano-6,7,10,11-tetraalkoxy-1,4-diazatriphenylenes and 2,3-dicyano-6,7,10,11-tetraalkoxytriphenylenes', Liquid Crystals, 34: 3, 401 — 410
To link to this Article: DOI: 10.1080/02678290601171428
URL: http://dx.doi.org/10.1080/02678290601171428

Liquid Crystals, Vol. 34, No. 3, March 2007, 401–410

Different disk structures in the hexagonal columnar mesophases of 2,3-dicyano-6,7,10,11-tetraalkoxy-1,4-diazatriphenylenes and 2,3-dicyano-6,7,10,11-tetraalkoxytriphenylenes

MASAHIRO ICHIHARA, HIROOMI SUZUKI, BERNHARD MOHR and KAZUCHIKA OHTA*

Smart Materials Science and Technology, Department of Bioscience and Textile Technology, Interdisciplinary Graduate School of Science and Technology, Shinshu University, 386-8567 Ueda, Japan

(*Received 8 August 2006; accepted 24 November 2006*)

We have synthesized two series of C_{2v} symmetric discotic liquid crystals of 2,3-dicyano-6,7,10,11-tetraalkoxy-1,4-diazatriphenylene [referred to as $(C_nO)_4$DADCT (**1**); n=8, 10, 12, 14] and 2,3-dicyano-6,7,10,11-tetraalkoxytriphenylene [referred to as $(C_nO)_4$DCT (**2**); n=8, 10, 12, 14]. Polarizing microscopic observations, differential scanning calorimetry and temperature-dependent X-ray diffraction studies revealed that each of the $(C_nO)_4$DADCT (**1**) and $(C_nO)_4$DCT (**2**) derivatives exhibits a hexagonal ordered columnar (Col_{ho}) mesophase, and that each of the $(C_nO)_4$DADCT (**1**) derivatives forms monomer disks in the Col_{ho} mesophase, whereas each of the $(C_nO)_4$DCT (**2**) derivatives forms dimer disks in the Col_{ho} mesophase. It is very interesting that the different disk structures may originate from the kind of atoms at the α-position to the CN groups in $(C_nO)_4$DADCT (**1**) and $(C_nO)_4$DCT (**2**).

1. Introduction

Discotic liquid crystals have attracted the interest of many liquid crystalline materials scientists since the discovery of discotic liquid crystals by Chandrasekhar in 1977 [1]. Recently, it has been expected the columnar structure of discotic liquid crystals could be applied to various electronic devices [2–6]. The most common mesophase in discotic liquid crystals is a hexagonal columnar (Col_h) mesophase. The Col_h mesophase is typically exhibited by D_{nh} (n=3, 4, 6) symmetric compounds. Generally, most of the discotic liquid crystalline compounds are substituted by six peripheral chains around the central core. These peripheral chains fulfil the space around the central core. Figure 1 shows examples of C_{2v} symmetric compounds A–D. Each of them has only four peripheral chains which are not enough to fill the space around the central core, but compounds A–C exhibit a columnar (Col) mesophase. In 1985, Wenz reported that compound A exhibits a Col mesophase [7]. Although he did not identify the mesophase of this compound, the mesophase may be a Col_h mesophase judging from the texture of the photomicrograph in his paper. In 1995, we reported for the first time that compound B exhibits a Col_{ho} mesophase in very wide temperature region, and that the Col_{ho} mesophase structure was established by temperature-dependent X-ray diffraction study [8]. In 2003, Williams and co-workers also reported the same homologues of compound B [9, 10]. In 1998, Rose and Meier reported that compound C exhibits a Col mesophase in very narrow temperature region, but they did not perform the detailed identification of the mesophase [11]. In 2002, Cammidge and Gopee reported that compound D does not exhibit any mesophase [12]. Thus, these compounds have very different temperature region of their columnar mesophases, although each of the compounds in figure 1 has the same symmetry (C_{2v}) with a slightly different molecular structure. Therefore, we would like to resolve this interesting problem.

In this study, we have systematically synthesized two series of C_{2v} symmetric discotic compounds of $(C_nO)_4$DADCT (**1a**–**1d**: n=8–14) and $(C_nO)_4$DCT (**2a**–**2d**: n=8–14) by the synthetic routes shown in scheme 1, to investigate their more detailed mesophase structures by precise temperature-dependent X-ray structural analyses. As described in the results section, each of the compounds **1** forms monomer disks in the Col_{ho} mesophase, whereas each of the compounds **2** forms dimer disks in the Col_{ho} mesophase. It should be emphasized that although the difference of the molecular structures between **1** and **2** is only the kind of two atoms in the central core, such an interesting disk structural difference was induced between these compounds. We wish to report here that these C_{2v} symmetric discotic liquid crystals, **1** and **2**, have

*Corresponding author. Email: ko52517@giptc.shinshu-u.ac.jp

Liquid Crystals
ISSN 0267-8292 print/ISSN 1366-5855 online © 2007 Taylor & Francis
http://www.tandf.co.uk/journals
DOI: 10.1080/02678290601171428

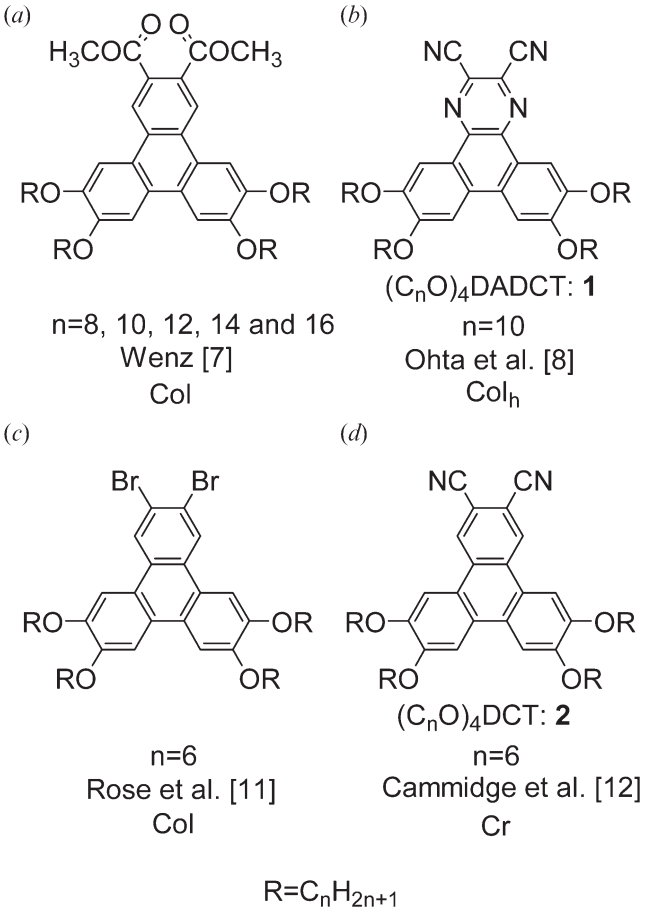

Figure 1. Discotic liquid crystalline molecular structures with C_{2v} symmetry. (Col=columnar mesophase, Col_h=hexagonal columnar mesophase, Cr=crystal).

different disk structures in the Col_{ho} mesophases, and that the disk structures greatly affect their mesophase temperature region.

2. Experimental

2.1. *Synthesis*

Scheme 1 shows the synthetic routes of $(C_nO)_4$DADCT (**1**) and $(C_nO)_4$DCT (**2**). $(C_nO)_4$DADCT (**1a**–**1d**) (n=8–14) was synthesized by our method [8, 13]. $(C_nO)_4$DCT (**2a**–**2d**) (n=8–14) was synthesized by the method of Cammigde and Gopee [12, 14]. Detailed procedures are described below for the representative $(C_{14}O)_4$DADCT (**1d**) and $(C_{12}O)_4$DCT (**2c**) derivatives.

2.1.1. 3,3′,4,4′-Tetramethoxybenzoin (3). Into a 300 ml three-neck flask, 3,4-dimethoxybenzaldehyde (30.0 g, 180 mmol), potassium cyanide (7.50 g, 115 mmol), ethanol (50 ml) and water (50 ml) were placed and the mixture was refluxed for 3 h. After cooling to room temperature, the reaction mixture was extracted with chloroform, washed with water and dried over anhydrous sodium sulfate. Then the solvent was evaporated. The purification of the crude product was performed by column chromatography (silica gel, chloroform, Rf=0.25) to give 20.2 g of yellow syrup. Yield=67%. IR (liquid film, cm^{-1}): 3450, 2950, 2850, 1660, 1590, 1505, 1270. ^{1}H NMR ($CDCl_3$, TMS): δ=3.43–4.50 (m, 13H, –OCH_3 and OH), δ=5.76–7.46 (m, 7H, Ar).

2.1.2. 3,3′,4,4′-Tetramethoxybenzil (4). Pyridine (120 ml), 3,3′,4,4′-tetramethoxybenzoin (20.0 g, 60.3 mmol), copper(II) sulfate pentahydrate (45.0 g, 180 mmol) and water (80 ml) were placed in a 300 ml three-neck-flask and the mixture was refluxed for 15 h. After cooling to room temperature, cold water (100 ml) was added to the reaction mixture to precipitate the target compound. The resulted precipitate was collected by filtration, washed with water until the filtrate became colorless. Then the compound was washed with THF and dried under vacuum to give 9.70 g of yellow crystals. Yield=50%, mp=223–224°C. IR (KBr, cm^{-1}): 2950, 2850, 1660, 1590, 1510, 1270. ^{1}H NMR ($CDCl_3$, TMS): δ=3.88 (s, 12H, –OCH_3), δ=6.73–7.50 (m, 6H, Ar).

2.1.3. 3,3′,4,4′-Tetrahydroxybenzil (5). Glacial acetic acid (50 ml), 47% hydrobromic acid (50 ml) and 3,3′,4,4′-tetramethoxybenzil (6.00 g, 18.1 mmol), were placed into a 300 ml three-neck flask and refluxed for 16 h. After cooling to room temperature, the reaction mixture was extracted with ether and neutralized with diluting sodium hydroxide aqueous solution. The organic layer was washed with water and dried over anhydrous sodium sulfate. The solvent was evaporated. The crude product was recrystallization from water to give 4.33 g of yellow solid. Yield=84%. IR (KBr, cm^{-1}): 3350, 1650, 1595, 1510, 1300.

2.1.4. 3,3′,4,4′-Tetrakis(tetradecyloxy)benzil (6d). Into a 300 ml three-neck flask, 3,3′,4,4′-tetrahydroxybenzil (1.50 g, 5.47 mmol), 1-bromotetradecane (9.98 g, 36.0 mmol), anhydrous potassium carbonate (4.32 g, 31.3 mmol) and dry *N*,*N*-dimethylacetamide (40 ml) were placed and the mixture was stirred at 70°C under nitrogen atmosphere for 7 h. The reaction mixture was extracted with chloroform, washed with water and dried over anhydrous sodium sulfate. Then the solvent was evaporated. The crude product was purified by recrystallization from ethyl acetate and hexane, respectively, to give 4.18 g of white solid. Yield=72%, mp=95°C. IR (KBr, cm^{-1}): 2930, 2860, 1670, 1590,

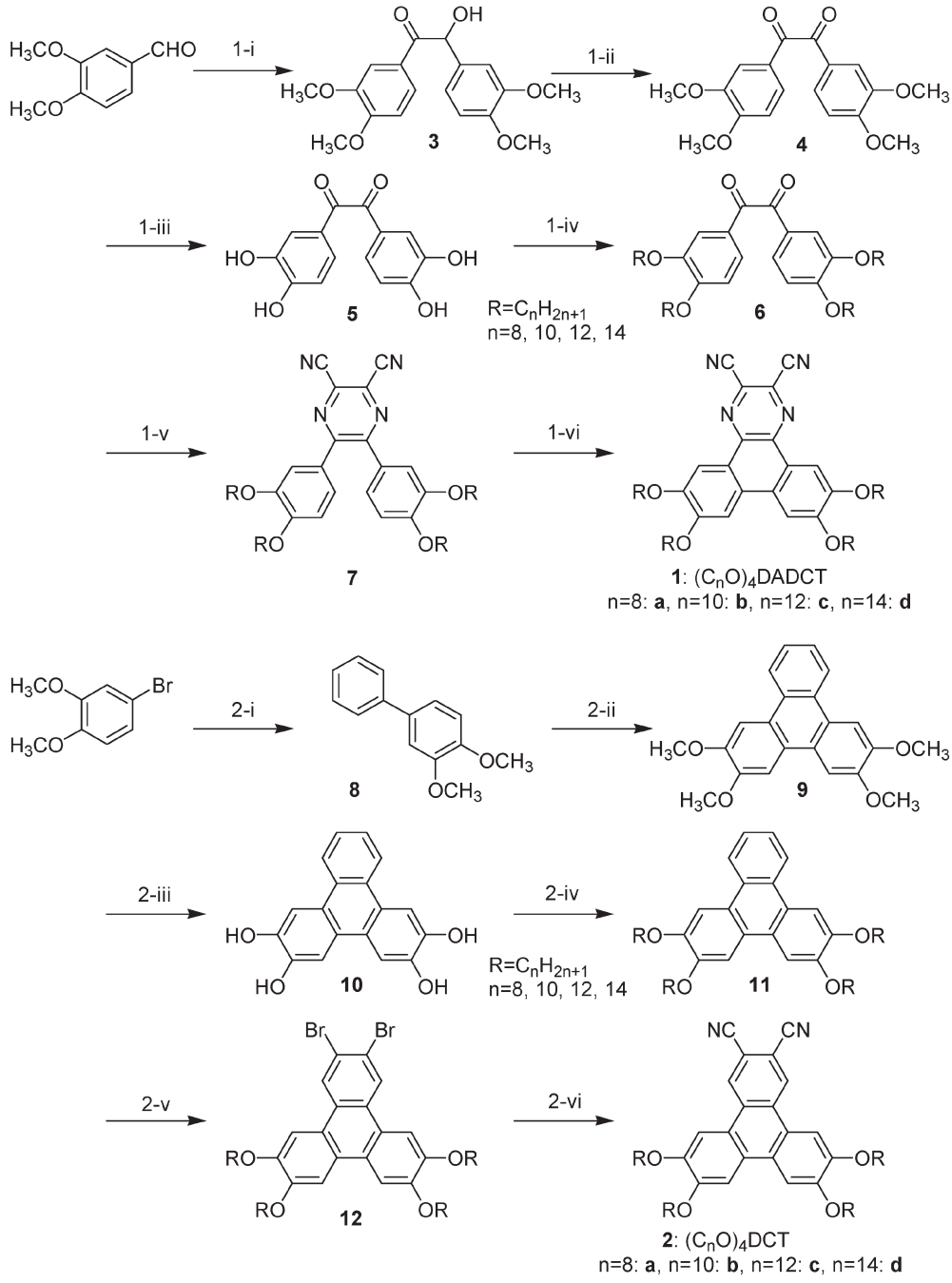

Scheme 1. Synthetic routes for 2,3-dicyano-6,7,10,11-tetraalokoxytriphenylene [**1**, $(C_nO)_4$DADCT] and 2,3-dicyano-6,7,10,11-tetraalkoxy-1,4-diazatriphenylene [**2**, $(C_nO)_4$DCT] (1-i: KCN, H_2O and MeOH; 1-ii: $CuSO_4.5H_2O$, H_2O and MeOH; 1-iii: CH_3COOH and HBr; 1-iv: RBr, K_2CO_3 and DMF; 1-v: diaminomaleonitril and CH_3COOH; 1-vi: VOF_3, BF_3 Et_2O and CH_2Cl_2; 2-i: $PhB(OH)_2$, toluene, H_2O and MeOH; 2-ii: 1,2-dimethoxybenzene, CH_2Cl_2 and $FeCl_3$; 2-iii: CH_3COOH and HBr; 2-iv: RBr, K_2CO_3 and DMF; 2-v: Br_2 and CH_2Cl_2; 2-vi: CuCN and DMF).

1510, 1270. ^{1}H NMR ($CDCl_3$, TMS): δ=0.87 (t, J=7.01, 12H, $-CH_3$), δ=1.29–1.81 (m, 72H, $-CH_2-$), δ=4.00 (t, J=6.65, 8H, OCH_2-), δ=6.64–7.74 (m, 6H, Ar).

2.1.5. 5,6-Bis(3,4-bis(tetradecyloxy)phenyl)-2,3-dicyanopyrazine (7d**).** Glacial acetic acid (100 ml), 3,3′,4,4′-tetrakis(tetradecyloxy)benzil (4.20 g, 3.96 mmol) and diaminomaleonitrile (0.630 g, 5.83 mmol) were placed

in a 300 ml three-neck flask and the mixture was refluxed under nitrogen atmosphere for 24 h. After cooling to room temperature, the reaction mixture was extracted with chloroform. The organic layer was washed with water and dried over anhydrous sodium sulfate. Then the solvent was evaporated. The purification of the crude product was performed by column chromatography (silica gel, chloroform, Rf=0.70) and recrystallization from acetone to give 3.16 g of yellow powder. Yield=71%, mp=75°C. IR (KBr, cm^{-1}): 2920, 2860, 2230, 1580, 1490, 1460. ^1H NMR ($CDCl_3$, TMS): δ=0.87 (t, J=7.02, 12H, $-CH_3$), δ=1.24 (m, 72H, $-CH_2-$), δ=3.80–3.93 (m, 8H, OCH_2-), δ=6.52–7.02 (m, 6H, Ar).

2.1.6. 2,3-Dicyano-6,7,10,11-tetrakis(tetradecyloxy)-1,4-diazatriphenylene (1d**).** Into a 200 ml recovery-flask, 5,6-bis(3,4-ditetradecyloxyphenyl)-2,3-dicyanopyrazine (3.00 g, 2.65 mmol) and dry dichloromethane (55 ml) were placed. Vanadium(V) trifluoride oxide (0.895 g, 7.22 mmol) and diethyl ether–boron trifluoride complex (0.718 g, 7.22 mmol) were added to the solution. The reaction mixture was stirred at room temperature for 90 min, followed by the addition of 5% citric acid. The mixture was extracted with dichloromethane, washed with water, dried over anhydrous sodium sulfate and evaporated to dryness. The crude compound was purified by column chromatography (silica gel, chloroform:hexane=5:2 (v/v), Rf=0.68) and recrystallization from hexane, ethyl acetate and acetone, respectively, to give 0.991 g of yellow solid. Yield=33%, mp=68.8°C. C.p.=224.2°C. IR (KBr, cm^{-1}): 2920, 2845, 2227, 1600, 1520, 1450. ^1H NMR ($CDCl_3$, TMS): δ=0.87 (t, J=7.00, 12H, CH_3), δ=1.27 (m, 72H, CH_2), δ=4.30 (t, J=6.62, 8H, OCH_2), δ=7.71–8.47 (m, 4H, Ar).

2.1.7. 3,4-Dimethoxybiphenyl (8**).** Phenylboronic acid (2.80 g, 0.0230 mol), 4-bromo-1,2-dimethoxybenzene (2.50 g, 0.0115 mol), potassium carbonate anhydrate (3.66 g, 0.0345 ml), palladium(II) chloride (0.0612 g, 0.345 mmol) and triphenylphosphine (0.181 g, 0.690 mmol) were stirred under reflux in a mixed solvent (toluene:ethanol:water=3:3:1, 15 ml) for 48 h. The solvent was evaporated. The crude product was extracted with chloroform and washed with water. The organic layer was dried over anhydrous sodium sulfate and the solvent was evaporated. The crude product was purified by column chromatography (silica gel, chloroform, Rf=0.60) and recrystallization from methanol to give 1.62 g of white crystals. Yield=66%, mp=71.1–71.4°C. IR (KBr, cm^{-1}); 2835, 2937, 2962, 1252, 1217, 1175, 1143, 761, 705. ^1H NMR (TMS/$CDCl_3$, ppm); δ=3.92 (s, 3H, OCH_3), δ=3.95 (s, 3H, OCH_3), δ=6.95 (d, J=8.08, 1H, Ar), δ=7.14 (m, 2H, Ar), δ=7.33 (t, J=1.14, 1H, Ar), δ=7.42 (t, J=7.70, 2H, Ar), δ=7.56 (q, J=8.22, 2H, Ar).

2.1.8. 2,3,6,7-Tetramethoxytriphenylene (9**).** 1,2-Dimethoxybenzene (2.00 g, 14.0 mmol) and 2,3-dimethoxybiphenyl (0.750 g, 3.49 mmol) were dissolved in dichloromethane (50 ml), then iron(III) chloride (4.46 g, 27.5 mmol) was rapidly added to the mixture. The mixture was stirred at room temperature for 2 h. The reaction mixture was treated with methanol followed by water, extracted with chloroform and washed with water. The organic layer was dried over anhydrous sodium sulfate and the solvent was evaporated. The purification of the crude product was performed by column chromatography (silica gel, chloroform, Rf=0.40) and recrystallization from ethanol two times to give 0.642 g of white crystals. Yield=53%, mp=214°C. IR (KBr, cm^{-1}); 2835, 2937, 2963, 1262, 1215, 1195, 1157, 845, 785, 753, 597. ^1H NMR (TMS/$CDCl_3$, ppm); δ=4.10 (s, 6H, OCH_3), δ=4.09 (s, 6H, OCH_3), δ=7.58 (q, J=6.32, 2H, Ar), δ=7.70 (s, 2H, Ar), δ=7.93 (s, 2H, Ar), δ=8.45 (q, J=6.32, 2H, Ar).

2.1.9. 2,3,6,7-Tetrahydroxytriphenylene (10**).** Glacial acetic acid and 47% hydrobromic acid (48.0 ml, 0.184 mmol) 2,3,6,7-tetramethoxytriphenylene (0.621 g, 1.70 mmol) were refluxed for 24 h. The reaction mixture was extracted with ethyl acetate and washed with water. The organic layer was dried over anhydrous sodium sulfate and the solvent was evaporated to give 0.510 g of brown solid. The compound was not purified since confirmation of the purity was very difficult due to decomposition at ca. 290°C. Yield=98%. IR (silicon wafer, cm^{-1}); 3299, 1600, 1529, 867, 855, 807, 769. ^1H NMR (TMS/C_3D_6O, ppm); δ=3.01 (s, OH), δ=7.49 (q, J=6.32, 1H, Ar), δ=7.88 (s, 1H, Ar), δ=8.07 (s, 1H, Ar), δ=8.43 (q, J=6.08, 1H, Ar).

2.1.10. 2,3,6,7-Tetrakis(dodecyloxy)triphenylene (11c**).** 1-Bromododecane (16.6 g, 66.5 mmol), 2,3,6,7-tetrahydroxytriphenylene (0.730 g, 2.50 mmol), dry ethanol (15 ml) and potasium carbonate anhydride (9.19 g, 6.5 mmol) were refluxed for 24 h. The reaction mixture was evaporated. The crude product was extracted with dichloromethane and washed with water. The organic layer was dried over anhydrous sodium sulfate and the solvent was evaporated. The crude product was purified by recrystallization from hexane to give 1.89 g of white solid. Yield=78%, mp=91–92°C. IR(KBr, cm^{-1}); 2850, 2921, 1616, 1264,

Table 1. Elemental analysis data of $(C_nO)_4$DADCT (**1**; n=8, 10, 12, 14) and $C_nO)_4$DCT (**2**; n=8, 10, 12, 14).

		Elemental analysis: found (calcd.)/%		
Compound	Mol. formula (Mol. wt)	N	C	H
1a $(C_8O)_4$DADCT	$C_{50}H_{72}N_4O_4$ (792.56)	7.09 (7.06)	75.79 (75.72)	8.87 (9.15)
1b $(C_{10}O)_4$DADCT	$C_{58}H_{88}N_4O_4$ (905.34)	6.11 (6.19)	76.63 (76.95)	9.45 (9.80)
1c $(C_{12}O)_4$DADCT	$C_{66}H_{104}N_4O_4$ (1017.56)	5.39 (5.51)	77.74 (77.90)	10.11 (10.30)
1d $(C_{14}O)_4$DADCT	$C_{74}H_{120}N_4O_4$ (1129.77)	4.95 (4.96)	78.37 (78.67)	10.43 (10.71)
2a $(C_8O)_4$DCT	$C_{52}H_{74}N_2O_4$ (791.16)	3.61 (3.54)	78.88 (78.94)	9.42 (9.43)
2b $(C_{10}O)_4$DCT	$C_{60}H_{90}N_2O_4$ (903.37)	3.19 (3.10)	80.01 (79.77)	10.36 (10.04)
2c $(C_{12}O)_4$DCT	$C_{68}H_{106}N_2O_4$ (1015.58)	2.72 (2.76)	80.10 (80.42)	10.09 (10.52)
2d $(C_{14}O)_4$DCT	$C_{76}H_{122}N_2O_4$ (1127.79)	2.38 (2.48)	80.83 (80.94)	11.05 (10.90)

1179, 838, 747, 724, 619. ^{1}H NMR (TMS/$CDCl_3$, ppm); δ=0.878 (t, J=6.84, 12H, CH_3), δ=1.27–2.17 (m, 80H, –CH_2–), δ=4.22 (t, J=6.32, 4H, OCH_2–), δ=4.23 (t, J=6.44, 4H, OCH_2–), δ=7.58 (q, J=6.08, 2H, Ar), δ=7.69 (s, 2H, Ar), δ=7.92 (s, 2H, Ar), δ=8.44 (q, J=6.20, 2H, Ar).

2.1.11. 2,3-Dibromo-6,7,10,11-tetrakis(dodecyloxy) triphenylene (12c**).** A mixture of 2,3,6,7-tetrakis(dodecyloxy)triphenylene (2.50 g, 2.59 mmol) and dry dichloromethane (50 ml) was stirred in ice–salt bath. Bromine (2.50 g, 2.59 mmol) in 50 ml of dichloromethane was added dropwise to the reaction mixture. The reaction mixture was stirred at 0 to −5°C in ice–salt bath for 4 h. The residual bromine was treated with sodium thiosulfate aqueous solution and then the organic layer was extracted with dichloromethane and washed with water. The organic layer was dried over anhydrous sodium sulfate and evaporated. The crude product was purified by precipitation from chloroform and excess ethanol and recrystallization from dichloromethane to give 0.898 g of white solid. Yield=78%, mp=96°C. IR (KBr, cm^{-1}); 2851, 2922, 2951, 1615, 1265, 1180, 837, 725. ^{1}H NMR (TMS/$CDCl_3$, ppm); δ=0.879 (t, J=6.82, 12H, CH_3), δ=1.27–1.96 (m, 80H, –CH_2–), δ=4.22 (t, J=6.32, 4H, OCH_2–), δ=4.23 (t, J=6.44, 4H, OCH_2–), δ=7.76 (s, 2H, Ar), δ=7.79 (s, 2H, Ar), δ=8.61 (s, 2H, Ar).

2.1.12. 2,3-Dicyano-6,7,10,11-tetrakis(dodecyloxy)triphenylene (2c**).** 2,3-Dibromo-6,7,10,11-tetrakis-(dodecyloxy)triphenylene (1.00 g, 0.890 mmol), CuCN (0.478 g, 5.34 mmol) and dry DMF (15 ml) were refluxed for 20 h. After cooling to room temperature, 25% aqueous ammonia solution was added to reaction mixture. The precipitate was collected by filtration and washed with water. The crude product was purified by recrystallization from dichloromethane and THF respectively to give 0.353 g of yellow crystal. Yield=39%, mp=142°C. cp=190C. IR (KBr, cm^{-1}); 2851, 2922, 2223, 1615, 1265, 1180, 837, 720. ^{1}H NMR (TMS/$CDCl_3$, ppm); δ=0.878 (t, J=6.82, 12H, –CH_3), δ=1.27–1.96 (m, 80H, –CH_2–), δ=4.22 (t, J=6.32, 4H, OCH_2–), δ=4.23 (t, J=6.44, 4H, OCH_2–), δ=7.80 (s, 2H, Ar), δ=7.87 (s, 2H, Ar), δ=8.85 (s, 2H, Ar).

2.2. *Measurements*

The compounds synthesized here were identified with a ^{1}H NMR (BRUKER Ultrashield 400 M Hz), an FT-IR (Nicolet NEXUS 670) and an elemental analyzer (Perkin-Elmer elemental analyzer 2400). The elemental analysis data are summarized in table 1. The phase transition temperatures and enthalpy changes were measured with a differential scanning calorimeter (Shimadzu DSC-50). The textures of their mesophases were observed with a polarizing optical microscope (Nikon ECLIPSE E600 POL) equipped with a Mettler FP82HT hot stage and a Mettler FP90 Central Processor. Wide-angle X-ray diffraction measurements were carried out with Cu-Kα radiation with a Rigaku RAD X-ray diffractometer equipped with a handmade heating plate [15, 16] controlled with a thermoregulator.

3. Results and discussion

3.1. *Mesomorphic behaviour*

Table 2 lists the phase transition temperatures and enthalpy changes of $(C_nO)_4$DADCT (**1**) and $(C_nO)_4$DCT (**2**). As can be seen from this table, each of the $(C_nO)_4$DADCT (**1a**–**1d**) and $(C_nO)_4$DCT (**2a**–**2d**) derivatives shows one or two crystalline phases, a Col_{ho} mesophase and an isotropic liquid (IL) phase.

Figures 2a and 2b show photomicrographs of the Col_{ho} mesophases of $(C_{12}O)_4$DADCT (**1c**) at 230°C and $(C_{12}O)_4$DCT (**2c**) at 176°C, respectively. As can be seen from these photomicrographs, each shows a dendric texture with C_6 symmetry. Generally, textures are contributed by symmetry of mesomorphic structures [17]. Hence, each of them could be identified as a Col_h mesophase. Each of the other mesophases of the

Table 2. Phase transition temperatures, T, and enthalpy changes, ΔH, of $(C_nO)_4$DADCT (**1**; n=8, 10, 12, 14) and $C_nO)_4$DCT (**2**; n=8, 10, 12, 14).

Compound	Phase T/°C (ΔH/kJ mol^{-1})↔Phase
1a $(C_8O)_4$DADCT	Cr_1 64.3 (5.83)↔Cr_2 84.8 (103)↔Col_{ho} 272.1 (6.74)↔IL
1b $(C_{10}O)_4$DADCT	Cr_1 62.1 (5.68)↔Cr_2 82.4 (69.7)↔Col_{ho} 256.4 (7.41)↔IL
1c $(C_{12}O)_4$DADCT	Cr_1 62.6 (3.92)↔Cr_2 74.1 (75.1)↔Col_{ho} 240.5 (7.29)↔IL
1d $(C_{14}O)_4$DADCT	Cr_1 44.6 (4.74)↔Cr_2 68.8 (93.8)↔Col_{ho} 224.2 (6.44)↔IL
2a $(C_8O)_4$DCT	Cr 183.2 (55.7)↔Col_{ho} 187.2 (3.43)↔IL
2b $(C_{10}O)_4$DCT	Cr_1 95.8 (6.81)↔Cr_2 164.1 (59.3)↔Col_{ho} 190.3 (4.29)↔IL
2c $(C_{12}O)_4$DCT	Cr_1 89.3 (7.30)↔Cr_2 141.9 (57.7)↔Col_{ho} 190.1 (3.88)↔IL
2d $(C_{14}O)_4$DCT	Cr_1 85.0 (13.4)↔Cr_2 121.4 (46.2)↔Col_{ho} 189.8 (4.20)↔IL

Phase nomenclature: Cr=crystal; Col_{ho}=hexagonal columnar ordered mesophase; IL=isotropic liquid.

$(C_nO)_4$DADCT (**1a**, **1b**, **1d**) and $(C_nO)_4$DCT (**2a**, **2b**, **2d**) derivatives (n=8, 10, 14) gave the same dendric texture.

In figure 3, the phase transition temperatures ere plotted against the number of carbon atoms in the peripheral chains. As can be seen from this figure, the mesomorphic temperature region of $(C_nO)_4$DADCT (**1a**–**1d**) is significantly wider than that of $(C_nO)_4$DCT (**2a**–**2d**). Furthermore, the clearing points of $(C_nO)_4$DADCT (**1**) drop with an increase in the number of carbon atoms in the peripheral chain. This is a common phenomenon for discotic liquid crystals. Contrary to the common phenomenon, the clearing points of $(C_nO)_4$DCT (**2**) are constant around 190°C, irrespective of the number of carbon atoms in the peripheral chain. An explanation of this will be provided in section 3.3.

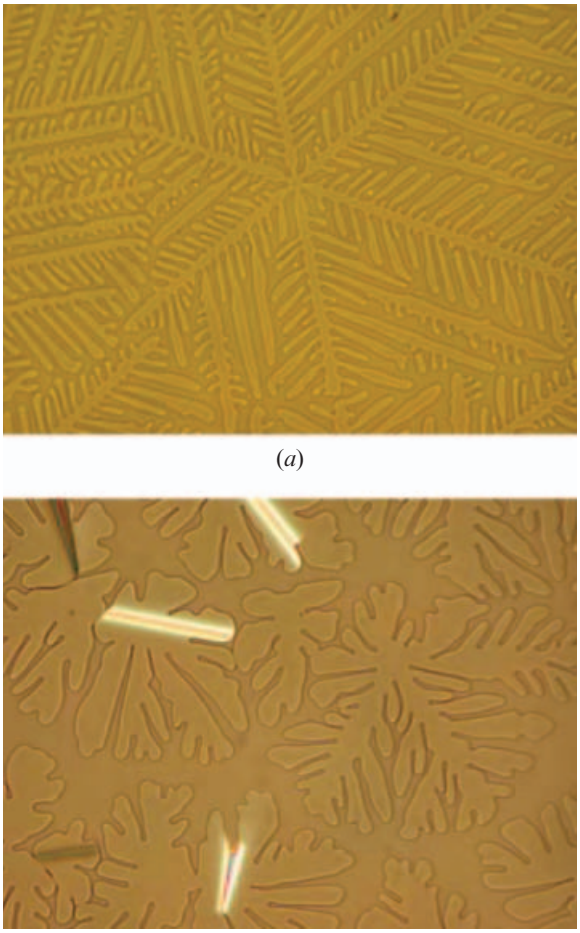

(*a*)

(*b*)

Figure 2. Photomicrographs of (a) $(C_{12}O)_4$DADCT (**1c**) at 230°C and (b) $(C_{12}O)_4$DCT (**2c**) at 176°C.

3.2. *Establishment of unique disk structures*

Temperature-dependent X-ray diffraction (XRD) studies were performed to reveal more precise mesophase structures. Figures 4a and 4b show the representative XRD patterns of $(C_{12}O)_4$DADCT (**1c**) and $(C_{12}O)_4$DCT (**2c**), respectively. As can be seen from figure 4a, the XRD pattern of $(C_{12}O)_4$DADCT (**1c**) shows three sharp peaks in the small-angle region, and a halo due to the molten alkoxy chains and a relatively sharp peak corresponding to the intracolumnar stacking distance in the wide angle region. The spacing ratio of these three sharp peaks in the small-angle region was $1:1/\sqrt{3}:1/2$ and these spacing values were well fitted to the Miller indices, (100), (110) and (200), of a 2-dimensional hexagonal lattice. Hence, the mesophase was identified as a hexagonal ordered columnar (Col_{ho}) mesophase. The lattice constant, a, of the 2-dimensional hexagonal lattice was calculated to be 25.0 Å (table 3). The number (Z) of molecules per a slice volume ($V=\sqrt{3}a^2h/2$) in the column could be calculated to be about 1 from the lattice constant (a=25.0 Å) and the intracolumnar stacking distance (h=3.46 Å). The value $Z\approx1$ clearly indicates that $(C_{12}O)_4$DADCT (**1c**) forms monomer disks in the slice volume (V) in the columns. Each of the other $(C_nO)_4$DADCT (**1a**, **1b**, **1d**) derivatives also exhibited the same XRD pattern and form monomer disks in the Col_{ho} mesophase.

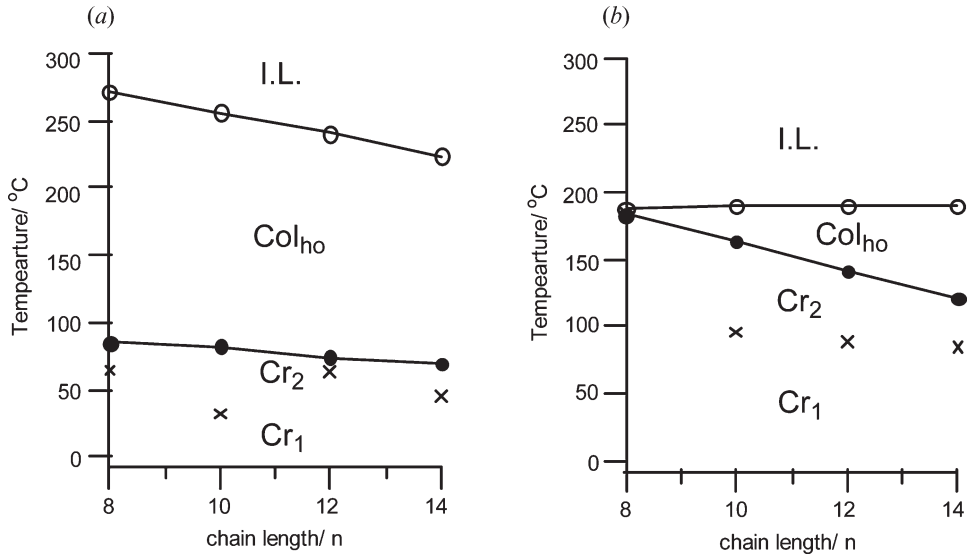

Figure 3. Relationships of the phase transition temperature and the chain length of (a) $(C_nO)_4$DADCT (**1**) and (b) $(C_nO)_4$DCT (**2**).

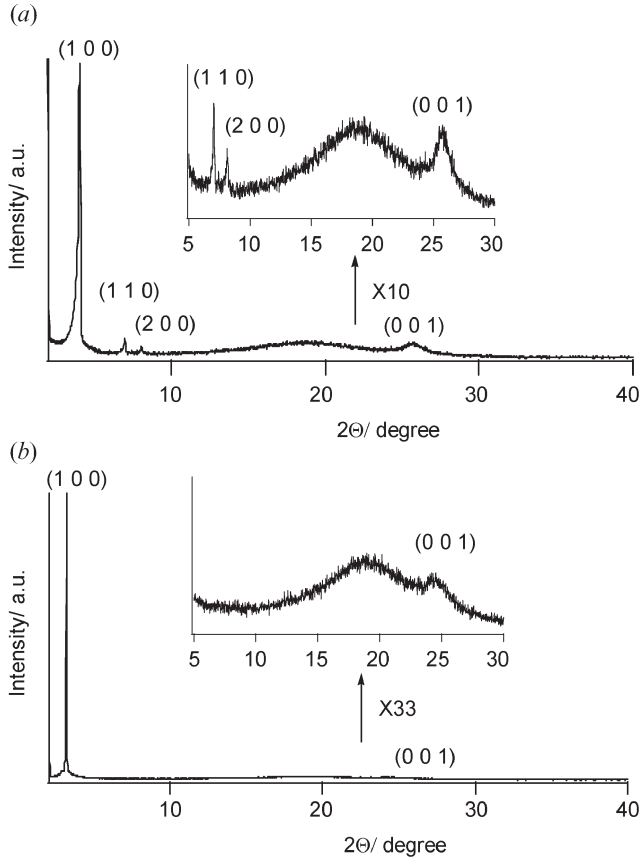

Figure 4. Representative temperature-dependent X-ray patterns. (a) $(C_{12}O)_4$DADCT (**1c**) at 120°C. (b) $(C_{12}O)_4$DCT (**2c**) at 170°C.

As can be seen from figure 4b, the XRD pattern of $(C_{12}O)_4$DCT (**2c**) shows one sharp peak in the small-angle region and a halo due to the molten alkoxy chains and a relatively broad peak corresponding to the intra-columnar stacking distance in the wide-angle region. Since the XRD pattern had only one peak in the small-angle region, the mesophase could not be identified only from this XRD study. However, as mentioned above, this mesophase shows a dendric texture having C_6 symmetry characteristic to a Col_h mesophase. Hence, the mesophase could be unambiguously identified as a Col_{ho} mesophase. From the spacing of one shape peak in the X-ray small angle region, the lattice constant, a, of the Col_{ho} mesophase could be calculated to be 33.1 Å. The Z value for this Col_{ho} mesophase was calculated to be about 2 from the lattice constant (a=33.1 Å) and the stacking distance (h=3.64 Å). The value $Z\approx2$ clearly indicates that $(C_{12}O)_4$DCT (**2c**) forms dimer disks in the slice volume ($V=\sqrt{3}a^2h/2$) in the columns. Each of the other $(C_nO)_4$DCT (**2a**, **2b**, **2d**) derivatives also exhibited the same XRD pattern and form dimer disks in the Col_{ho} mesophase.

The XRD data of all the compounds are listed in table 3. As can be seen from this table, each of the lattice constants, a, of $(C_nO)_4$DCT (**2a**–**2d**) is longer than that of $(C_nO)_4$DADCT (**1a**–**1d**) (for n=8, Δa=5.9Å; n=10, Δa=5.9 Å (7.0 Å); n=12, Δa=8.1 Å; n=14, Δa=6.9 Å). The differences (Δa) between the lattice constants, a, of these two series of the compounds **1** and **2** are 6–8 Å, which is almost the same length as a triphenylene core diameter (7.1 Å). Figure 5 illustrates the possible disk shapes of $(C_nO)_4$DADCT (**1**) and $(C_nO)_4$DCT (**2**) in the

Table 3. X-ray data of $(C_nO)_4$DADCT (n=8, 10, 12 and 14) and $(C_nO)_4$DCT (n=8, 10, 12 and 14).

Compound	Mesophase lattice constants/Å	Spacing/Å		Miller indices (h k l)
		Observed	Calculated	
1a: $(C_8O)_4$DADCT	Col_{ho} at 120°C	19.1	19.1	(1 0 0)
	a=22.1	11.0	11.0	(1 1 0)
	h=3.49	9.48	9.55	(2 0 0)
	Z=*ca.* 1 for ρ=1.00*	*ca.* 4.6	–	#
		3.49	–	h
1b: $(C_{10}O)_4$DADCT (This work)	Col_{ho} at 120°C	20.6	20.6	(1 0 0)
	a=23.9	11.8	11.7	(1 1 0)
	h=3.47	10.2	10.0	(2 0 0)
	Z=*ca.* 1 for ρ=1.00*	*ca.* 4.6	–	#
		3.47	–	h
1b: $(C_{10}O)_4$DADCT (Previous work)◇	Col_{ho} at 100°C	19.7	19.7	(1 0 0)
	a=22.8	11.6	11.4	(1 1 0)
	h=3.50	10.0	9.85	(2 0 0)
	Z=*ca.* 1 for ρ=1.00*	*ca.* 4.8	–	#
		3.50	–	h
1c: $(C_{12}O)_4$DADCT	Col_{ho} at 120°C	21.6	21.6	(1 0 0)
	a=25.0	12.5	12.5	(1 1 0)
	h=3.46	10.8	10.8	(2 0 0)
	Z=*ca.* 1 for ρ=1.00*	*ca.* 4.6	–	#
		3.46	–	h
1d: $(C_{14}O)_4$DADCT	Col_{ho} at 120°C	23.1	23.1	(1 0 0)
	a=26.7	13.4	13.3	(1 1 0)
	h=3.43	11.6	11.6	(2 0 0)
	Z=*ca.* 1 for ρ=1.00*	*ca.* 4.7	–	#
		3.43	–	h
2a: $(C_8O)_4$DCT	Col_{ho} at 185°C	24.1	24.1	(1 0 0)
	a=28.0	*ca.* 4.6	–	#
	h=3.62	3.62	–	h
	Z=*ca.* 2 for ρ=1.00*			
2b: $(C_{10}O)_4$DCT	Col_{ho} at 170°C	25.7	25.7	(1 0 0)
	a=29.8	*ca.* 4.6	–	#
	h=3.61	3.61	–	h
	Z=*ca.* 2 for ρ=1.00*			
2b: $(C_{10}O)_4$DCT	Col_{ho} at 170°C	28.5	28.5	(1 0 0)
	a=33.1	*ca.* 4.6	–	#
	h=3.64	3.64	–	h
	Z=*ca.* 2 for ρ=1.00*			
2b: $(C_{10}O)_4$DCT	Col_{ho} at 185°C	29.0	29.0	(1 0 0)
	a=33.6	*ca.* 4.6	–	#
	h=3.66	3.66	–	h
	Z=*ca.* 2 for ρ=1.00*			

#: Halo of molten alkoxy chains. * : Assumed density (g/cm^3). ◇: Previous work by Ohta et al. [8].

Col_{ho} mesophases. As can be seen from figure 5A, the disk diameter (a_1) of the monomeric $(C_nO)_4$DADCT (**1**) is equal to c+2p, because the monomer-disk diameter (a_1) is compatible with sum of the diameter of one triphenylene macrocycle (=c) and the length of two peripheral chains (=$p \times 2$). Two successive molecules of $(C_nO)_4$DADCT (**1**) may pile up in antiparallel way to fulfil the circular area illustrated in this figure. On the other hand, the disk diameter (a_2) of dimeric $(C_nO)_4$DCT (**2**) is equal to 2c+2p, because the dimer-disk diameter (a_2) should be longer by the diameter of one triphenylene macrocycle (=c) than the monomer-disk diameter (a_1) of $(C_nO)_4$DADCT (**1**), as illustrated in figure 5B: $a_2-a_1=(2c+2p)-(c+2p)=c$. This is consistent with the lattice

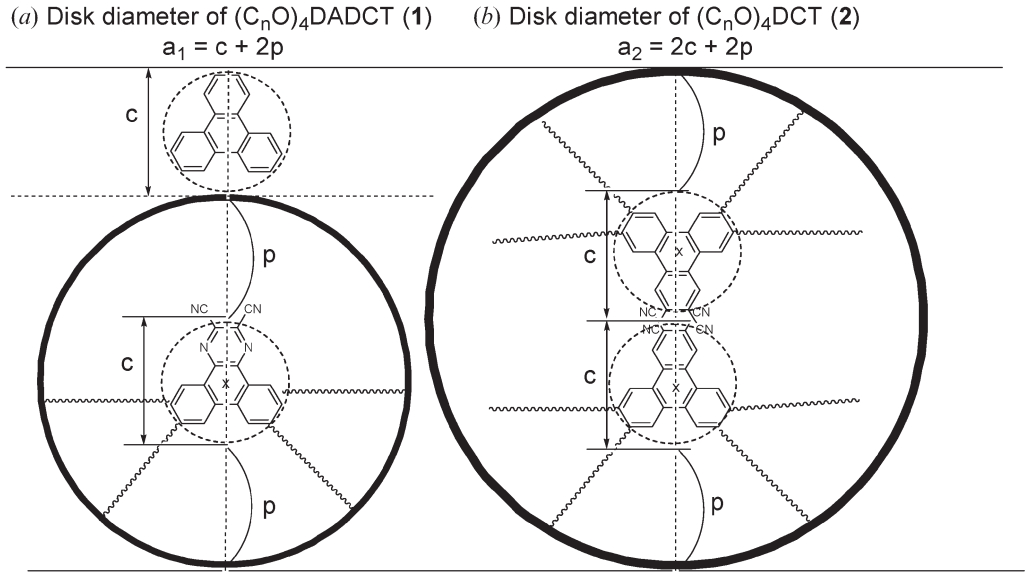

Figure 5. Schematic models of the columnar diameters: (A) diameter of monomer for $(C_nO)_4$DADCT (**1**); (B) diameter of dimer for $(C_nO)_4$DCT (**2**) (c=core diameter; p=length of the hydrocarbon chain; bold circle=disk dimension; dashed circle=core dimension).

constant differences Δa=6–8 Å mentioned above. Since $(C_nO)_4$DCT (**2**) forms dimer disks, the CN groups of the first $(C_nO)_4$DCT (**2**) molecule must face the CN groups of the second $(C_nO)_4$DCT (**2**) molecule, as illustrated in figure 5B. Additionally, the difference of the disk structures between **1** and **2** is also supported by the XRD reflection of intracolumnar distance in the wide angle region in figure 4. This reflection of **1** is sharp in comparison with that of **2**. This sharpness is related to the order of the stacking distance. The staking distance of the monomer disks should be more ordered than that of the dimer disks. This is compatible with the difference of the disk structures in columns.

The difference of the disk structures between **1** and **2** may be originate from the kind of atoms at α-position of the CN groups because the difference of the molecular structures between $(C_nO)_4$DADCT (**1**) and $(C_nO)_4$DCT (**2**) is only the nitrogen atoms in the core of **1**.

3.3. *Constant clearing points of the dimeric $(C_nO)_4$DCT (2) derivatives*

As mentioned above, the clearing points of $(C_nO)_4$DCT (**2a**–**2d**) are constant around 190°C. Generally, the fluctuation in a thermotropic mesophase increases with increasing peripheral chain length, so that the longer peripheral chain induces a lower clearing point. Hence, it is natural that a clearing point depends on a peripheral chain length, as for the clearing points of the $(C_nO)_4$DADCT (**1a**–**1d**) derivatives (see figure 3a). On the contrary, the clearing points of $(C_nO)_4$DCT (**2a**–**2d**) do not depend on the peripheral chain length but are constant around 190°C. As mentioned above, $(C_nO)_4$DCT (**2a**–**2d**) form dimer disks in the Col_{ho} mesophase. The dissociation of the dimers may occur at a certain temperature, so that the clearing points of $(C_nO)_4$DCT (**2a**–**2d**) do not depend on the peripheral chain length.

4. Conclusion

Two series of C_{2v} symmetric discogens $(C_nO)_4$DADCT (**1**) and $(C_nO)_4$DCT (**2**) (n=8, 10, 12, 14) have been synthesized. It was revealed by polarizing optical microscopic observation, differential scanning calorimetry and temperature-dependent X-ray diffraction studies that each of the $(C_nO)_4$DADCT (**1**) and $(C_nO)_4$DCT (**2**) derivatives exhibits a hexagonal ordered columnar mesophase (Col_{ho}), and that $(C_nO)_4$DADCT (**1**) and $(C_nO)_4$DCT (**2**) exist as monomer disks and dimer disks, respectively, in the Col_{ho} mesophase. Interestingly, the clearing points of $(C_nO)_4$DCT (**2a**–**2d**) are constant around 190°C, irrespective of the chain length. The dissociation of the dimer disks of $(C_nO)_4$DCT (**2**) may occur at a certain temperature, so that the clearing points of $(C_nO)_4$DCT (**2**) do not depend on the peripheral chain length.

Acknowledgements

This work was partially supported by a Grant-in-Aid for the 21st Century COE Program and a Grant-in-Aid for Science Research (18039013) in a Priority Area "Super-Hierarchical Structures" from the Japanese Ministry of Education, Culture, Sports, Science and Technology.

References

[1] S. Chandrasekhar. In *Handbook of Liquid Crystals*, Vol. 2B, D. Demus, J. Goodby, G.W. Gray, H.W. Spiess, Vill (Eds), pp. 749–798, Wiley-VCH (1998).
[2] D. Adam, P. Schuhmacher, J. Simmerer, L. Haussling, K. Siemensmeyer, K.H. Etzbach, H. Ringsdorf, D. Haarer. *Nature*, **371**, 141 (1994).
[3] N. Borden, R.J. Bushby, J. Clements, B. Monaghar. *Phys. Rev. B*, **52**, 274 (1995).
[4] K. Ohta, K. Hatsusaka, M. Sugibayashi, M. Ariyoshi, K. Ban, F. Maeda, R. Naito, K. Nishizawa, A.M. van de Craats, J.M. Warman. *Mol. Cryst. liq. Cryst.*, **397**, 25 (2003).
[5] A.M. van de Craats, N. Stutzmann, O. Bunk, M.M. Nielsen, M. Watson, K. Müllen, H.D. Chanzy, H. Surringhaus, R.H. Friend. *Adv. Mater.*, **15**, 495 (2003).
[6] W. Pisula, A. Menon, M. Stepputat, I. Lieberwirth, U. Kolb, A. Tracz, H. Sirringhaus, T. Pakula, K. Müllen. *Adv. Mater.*, **17**, 684 (2005).
[7] G. Wenz. *Markromol. Chem. Rapid Commun.*, **6**, 577 (1985).
[8] B. Mohr, G. Wegner, K. Ohta. *J. chem. Soc., chem. Commun.*, 995 (1995).
[9] J. Babuin, J. Foster, V.E. Williams. *Tetrahedron Lett.*, **44**, 7003 (2003).
[10] E.J. Foster, J. Babuin, N. Nguyen, V.E. Williams. *J. chem. Soc., chem. Commun.*, 2052 (2003).
[11] B. Rose, H. Meier. *Z. Naturforsch.*, **53b**, 1031 (1998).
[12] A.N. Cammidge, H. Gopee. *J. chem. Soc., chem. Cummun.*, 966 (2002).
[13] B. Mohr, V. Enkelman, G. Wegner. *J. org. Chem.*, **59**, 635 (1994).
[14] A.N. Cammidge, H. Gopee. *J. Mater. Chem.*, **11**, 2773 (2001).
[15] H. Hasebe. Masters Thesis, Shinshu University, Ueda, Chap. 5 (1991).
[16] H. Ema. Masters Thesis, Shinshu University, Ueda, Chap. 7 (1988).
[17] C. Baehr, M. Ebert, G. Frick, J.H. Wendorff. *Liq. Cryst.*, **7**, 601 (1990).